CEES 2020
12 – 15 OCTOBER 2021
COIMBRA | PORTUGAL
INTERNATIONAL CONFERENCE
CONSTRUCTION, ENERGY
ENVIRONMENT & SUSTAINABILITY

Alkali activation of electric arc furnace slag: Optimum concentration of the alkali activator and mechanical performance of mortars

Dany Kassim [1]
Rui Vasco Silva [1]
Jorge de Brito [1]

[1] CERIS, Instituto Superior Técnico, Universidade de Lisboa, Av. Rovisco Pais, 1049-001 | Lisboa, Portugal
Corresponding author: rui.v.silva@tecnico.ulisboa.pt

Keywords

Alkali-activated materials, Electric arc furnace slag, Mechanical performance, Mortars.

Abstract

In this study, electric arc furnace slag (EAFS) is examined as a potential full replacement of cement in the production of alkali-activated mortars. The EAFS used in this study, which is a by-product of steel manufacturing, was provided by HARSCO from the beneficiated output at Siderurgia Nacional, Portugal. Given its extensive particle size distribution, milling of the EAFS was required to achieve a cement-like sized powder before it could be used as a precursor in alkali activation. Different combinations of sodium hydroxide (NaOH) and sodium silicate (Na_2SiO_3) were tried, by varying the Na_2O/binder (4%; 6%; 8%; 10%; 12%) and SiO_2/Na_2O (0; 0.5; 1.0; 1.5; 2.0; 2.5) ratios, in order to maximize the mechanical performance. The alkaline activators were prepared 24 h before the mixing to attain a similar temperature for all mixes. The results showed that the SiO_2/Na_2O ratio and the compressive strength are directly proportional to each other. The maximum 28-day compressive strength obtained from this study, after being subjected to thermal curing for the first 24 hours at 80 °C, was 9.1 MPa in mixes with 4% and 2.5 MPa as Na_2O/binder and SiO_2/Na_2O ratios, respectively. However, after undergoing 28 days in an additional accelerated carbonation stage, the maximum compressive strength (i.e. 31 MPa from an initial 3.9 MPa in uncarbonated mixes, corresponding to an 800% increase) was obtained in mixes with 12% and 1.0 for Na_2O/binder and SiO_2/Na_2O ratios, respectively, thus showing a shift in the optimal alkaline activator contents. The complete replacement of cement with alkali-activated aluminosilicate wastes may translate into significant reductions in cost and minimal environmental impacts, especially with incorporating a forced carbon curing stage using industrial CO_2-rich flue gases.

1. INTRODUCTION

Almost 40% of the global production of steel is possible using the electric arc furnace (EAF) manufacturing process [1]. This technique corresponded to over 55% of the market in the United States in 2006 [2]. The EAF method utilizes scrap metal as its primary raw material, which is why it is considered a more sustainable and economical procedure [1]. Electric arc furnace slag (EAFS), a by-product of this process, corresponds to 15% to 20% of the steel production output [3]. In 2017, Brazil produced 34 million tonnes of steel and 9 million tonnes of EAFS [4]. This is an indication that large developing countries such as Brazil, Russia, India and China are producing large amounts of steel slag with little to no well-established outlet in the industry and thus additional efforts will have to be exerted to reintroduce this waste into supply chains. In this context, these materials could be used as alternatives in the construction industry, which is among the highest consumers of resources. There have been some studies on the use of EAFS as a substitute of natural aggregates for the production of concrete [5-7]. Cesnovar et al. [8] stated that alkali-activated slag-based materials are excellent alternatives to cement in civil works. EAFS, though somewhat different from conventional steel slag, also contains amorphous aluminates and silicates that can be activated using alkaline solutions. In this regard, EAFS offers the potential of replacing Portland cement, which is the primary source of CO_2 emission [9]. For instance, 1 tonne of Portland cement production emits 0.80-0.95 tonnes of CO_2 [9-13].

The experimental work described in this paper concerns the use of alkali-activated electric arc furnace slag (AAEAFS) as a precursor in mortars, focusing on optimizing the alkaline activator to achieve maximum mechanical performance. It describes the several stages, including the materials typically used to produce alkali-activated mortars (i.e. precursor, aggregates, and alkaline activators). It presents the mix design of all planned mortars and the testing methodology of fresh- and hardened-state mortars, including: slump; shrinkage; flexural strength (FS); compressive strength (CS); and carbonation. Twenty-one different mixes were produced to investigate the optimum concentration of the alkali activator in EAFS mortars. Different concentrations of sodium hydroxide (NaOH) and sodium silicate (Na_2SiO_3) were tested, by changing the Na_2O/binder (4%; 6%; 8%; 10%; 12%) and SiO_2/Na_2O (0; 0.5; 1.0; 1.5; 2.0; 2.5) ratios, to obtain the highest mechanical performance. The correlation between the various tested parameters was analysed to identify the optimum combination that yields the highest 28-day compressive strength and subsequently quantify the effect imposed by the accelerated carbonation process on the strength of AAEAFS mortars.

2. MATERIALS AND METHODS

2.1. ELECTRIC ARC FURNACE SLAG (EAFS)

EAFS is a by-product of steel manufacturing collected from the Siderurgia Nacional de Portugal, provided by HARSCO. It presents an extensive particle size distribution and requires preparation and grinding to be used as a binder. This material presents an apparent density of 3770 kg/m^3. The oxide chemical composition of the raw material, obtained from X-ray fluorescence (XRF), is shown in Table 1. This EAFS contains 28.5% of Fe_2O_3, 28.2% of CaO, 17.7% of SiO_2, and 10.1% of Al_2O_3. The high amount of iron in EAFS could induce magnetic properties on AAEAFS concrete [14]. Hafez et al. [15] stated that the amount of aluminosilicate is sufficient to allow this material to contribute as a binder. However, dimensional instability of concrete may occur due to the presence of CaO [16].

Table 1 - Chemical composition of EAFS (%)

Fe_2O_3	CaO	SiO_2	Al_2O_3	MgO	MnO_2	Cr_2O_3	TiO_2	P_2O_5	SO_3	Na_2O	BaO	K_2O	V_2O_5	CuO	ZnO
28.5	28.2	17.7	10.1	5.66	5.44	2.38	0.65	0.42	0.33	0.19	0.17	0.03	0.11	0.02	0.02

2.2. ALKALINE ACTIVATOR

The alkaline activator was prepared in the form of a liquid solution. Reactive grade anhydrous sodium hydroxide pellets (NaOH), with 98% purity and a density of 2.13 g/ml, then dissolved in a solvent: tap water complying with Directive 98/83/CE [17]. A commercial solution of sodium metasilicate was used, containing a sodium oxide (Na_2O) content of 8 ± 0.6%, silicon oxide (SiO_2) of 26.4 ± 1.5% and water content of 65.6 ± 2%. It presented a relative density of 1.355 g/ml.

2.3. FINE AGGREGATES

Two types of fine siliceous aggregates were used for mortar production. The first type was coarse sand 0/4, and the second type was fine sand 0/1. The bulk density, water absorption, humidity, and size were evaluated before using these fine aggregates, as shown in Table 2. The fine $sand_{0/1}$ ranged from 2 mm to ~0.06 mm, representing 30% of the total mass of aggregates within the mix. The coarse $sand_{0/4,}$ which corresponded to 70% of the total mass of aggregates in the mix had particle size distribution of 8 mm to ~0.06 mm.

2.4. WATER REDUCING ADMIXTURE

The water-reducing admixture (WRA) used in this campaign was SikaPlast-717, consisting of a synthetic organic water-based naphthalene-based dispersant, having a density of 1.21 ± 0.03 kg/dm^3 and a pH of 10 ± 1.

Table 2 - Characterization of the aggregates used in the mortar mixes

Aggregates	Nominal size	Oven-dried density	Water absorption	Mass ratio
	mm	kg/m^3	%	%
Fine sand	0/1	2637	0.4	30
Coarse sand	0/4	2617	0.5	70

2.5. MORTAR MIX DESIGN

The experimental campaign focused on optimizing the alkaline activator, which was carried out based on the mortar's mechanical performance. To achieve the optimum activator for EAFS, the Na_2O/precursor mass ratio varied between 0.04 and 0.12. The SiO_2/Na_2O ratio varies between 0 and 2.5. The same curing temperature and time of 80 °C and 24 hours, respectively, were applied to all mortars. The amount of each constituent was calculated based on volumetric and mass ratios of the components, using the density of each of the raw materials. The binder/aggregate volumetric ratio (V_B/V_A) was of 0.33. The mass ratio of SiO_2/Na_2O varied between 0, 0.5, 1.0, 1.5, 2.0, and 2.5. The mass ratio of water/binder (M_W/M_B) was fixed at 0.3. The mass WRA/precursor ratio varied from 0% to 1%, and the Na_2O/binder was of 4%, 6%, 8%, 10%, and 12% as shown in Table 3.

Table 3 - Matrix of 21 different families of AAEAFS mixes.

Na_2O/Precursor (%)	**SiO_2/Na_2O**					
	0.0	**0.5**	**1.0**	**1.5**	**2.0**	**2.5**
4	MS1	MS6	MS11	MS16	MS19	MS21
6	MS2	MS7	MS12	MS17	Ms20	*
8	MS3	MS8	MS13	MS18	*	*
10	MS4	MS9	MS14	*	*	*
12	MS5	MS10	MS15	*	*	*

2.6. PRODUCTION METHOD

Mortar production was based on EN 196-1 [18]. The alkaline solution was prepared by gradually dissolving the NaOH pellets in water and then left to cool down for 24 hours. The 40×40×160 mm^3 steel moulds were wrapped entirely in thin plastic film to eliminate the use of any releasing agent. The alkaline solution was added first in the mixer along with the WRA and the precursor and then mixed for 3 minutes. After that, the mixer was stopped until the fine aggregates were added, and then all the components were mixed for another 2 minutes, and one additional minute in higher mixing speed was applied. After that, the slump was tested on the slump table according to EN 1015-3 [19]. Afterwards, the mix was moulded and covered with plastic film and immediately placed in a thermal curing chamber at 80 °C for 24 hours. Finally, the specimens were demoulded. Each specimen was sealed and placed to cure in a dry chamber with a temperature of 23 ± 2 ºC and relative humidity of 65% until the testing day.

2.7. CURING CONDITIONS

After moulding the mortar and covering the steel moulds with plastic film, they were transported for thermal curing for 24 hours in the treatment oven at a temperature of 80 °C. At the end of this stage, the mortar specimens were demoulded and placed in their designated curing condition depending on the desired test method, as shown in Table 4**Error! Reference source not found.**.

Table 4 - Curing conditions, test methods and number of specimens of the experimental campaign

Test	Standard	Number of specimens	Curing conditions
Flexural strength Compressive strength	EN 1015-11 [20]	6	Specimens were placed sealed in a dry chamber until testing age.
Accelerated carbonation	EN 13295 [21]	4	14 days sealed and another 14 days unsealed in the dry chamber; then placed in the carbonation chamber until testing age.
Shrinkage	EN 1015-13 [22]	2	Specimens were placed in a dry chamber sealed after demoulding until the end of the test.

3. RESULTS AND DISCUSSION

3.1. WORKABILITY

The mortar's workability was evaluated by their slump according to the EN 1015-3 [19] standard. The superplasticizer was used and adjusted accordingly between 0% and 1.0% depending on the Na_2O/binder and SiO_2/Na_2O ratios. As the Na_2O/binder ratio increased, workability decreased. This was due to the higher viscosity of the alkaline solution after the addition of a solid solute. It was also expected that mixes would lose workability after a short time for higher SiO_2/Na_2O ratios due to the well-known flash setting; Ca^{2+} ions from the EAFS quickly react with the silicate ions of the solution, leading to the precipitation of an initial C-S-H, responsible for the setting [23]. Therefore, it can be stated that there is a correlation between workability and Na_2O/binder and SiO_2/Na_2O ratios. The target slump had been initially set at 140 ± 20 mm. However, mixes MS13, MS14 and MS15 presented a slightly lower slump between 109 mm and 117 mm due to the increase in viscosity of the alkaline activator. Therefore, the superplasticizer content increased to 1.0 % for mixes with silicate modulus ratio equal to or more than 1.5, to adjust the workability and slump to reach between 130 mm and 147 mm.

3.2. COMPRESSIVE STRENGTH

The average compressive strength of AAEAFS is presented in Figure 1, which shows how the different parameters significantly affect the property. Mixes MS6, MS7, MS9, and MS10 are to be repeated due to inconsistent values and unexpected outcomes during the mixing process. The alkaline solutions of mixes MS9 and MS10 showed precipitation, possibly due to the saturation of silica, during the 24 hours before the mixing day. Thus, the solution must be prepared again under different conditions to avoid any fluctuation in the results. Correspondingly, the alkali activator is the most important factor controlling compressive strength. Different studies on alkali-activated EAFS used at least one of the alkaline activators stated in this study; Turker et al. [24], Ozturk et al. [25], and Peys et al. [26] used both sodium hydroxide and sodium silicate to obtain compressive strength values of 40.7 MPa, 22.0 MPa, and 16.0 MPa, respectively, while Abdollahnejad et al. [27] used only sodium hydroxide and achieved 27.0 MPa. However, the maximum compressive strength in this study for uncarbonated specimens was of 9.61 MPa for mixes with 4% and 2.5 of Na_2O/binder and SiO_2/Na_2O ratios, respectively. Mixes MS4 and MS5, which were specimens with insufficient stability, exhibited values close to zero and thus are not presented here. This could be due to the excess amount of sodium hydroxide and the lack of sodium silicate. Increasing the amount of Na_2O until a given percentage increases the strength, after which the performance starts to deteriorate. Nevertheless, excess amount of OH^-, due to the $Ca(OH)_2$ across the particles of EAFS, reduces the interaction of Ca^{2+} ions from the surface of EAFS [28]. Therefore, it can be stated that the low strength results from the inadequate amount of C-S-H gels produced by the reaction of Ca^{2+} with Si^{4+}.

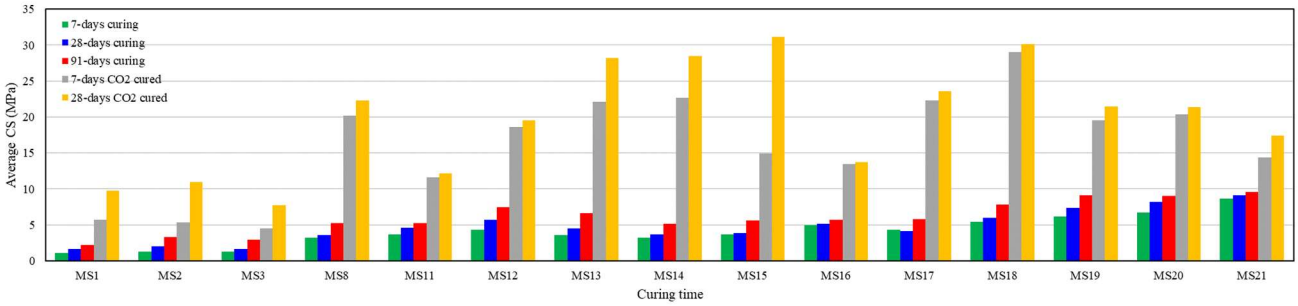

Figure 1 - Average compressive strength (CS)

Sodium hydroxide and sodium silicate have a significant influence on the mechanical properties of AAEAFS. Si^{4+} and Al^{3+} ions within the EAFS dissolve much more with a high concentration of OH^- [29]. Song et al. [30] observed that increasing the concentration of the alkali activator increases the reaction rate as a result of a high alkali medium. Wang et al. [31] stated that sodium hydroxide and sodium silicate are directly proportional to compressive strength only to a given level from 3-5% by weight of the mix. The authors also stated that, if the amount of sodium concentration increased over a given point, it would cause efflorescence. This is due to the migration of Na^+ ions to the surface of the specimens, leading to the precipitation of sodium carbonate.

Another parameter affecting the compressive strength for all mixes was time. The specimens in this study experienced 7-days, 28-days, and 91-days of curing time in a dry chamber at 23 ± 2 ºC. Since all specimens were sealed, there were no exchanges of humidity with the surrounding environment. The maximum compressive strength of the same alkali activator combination stated earlier in this section was obtained at 91-days of curing. However, the compressive strength has increased significantly by forcing CO_2 into the specimen, as detailed in section 3.4.

3.3. FLEXURAL STRENGTH

Figure 2 presents the results observed for the flexural strength of AAEAFS mortars. The maximum 28-day flexural strength for uncarbonated specimens achieved was 1.57 MPa for the same optimum mix as the one observed for compressive strength. However,

the surface of the specimens presented some microcracks. Ya-Min et al. [32] stated that this might be due to the heat curing process and the expedited nature of the reactions at relatively high-temperature levels, which may have induced a significant amount of microcracks, thereby resulting in reduced strength. Although a higher SiO_2/Na_2O ratio is a good indicator of an improved performance [29, 33-35], the low performance in the case of the EAFS may be due to the low amount of amorphous phases present in the precursor, which did not react with the alkaline activator. Furthermore, even though one would expect to have improved performance from the interaction of Ca from the EAFS with the SiO_2 from the activator to produce C-S-H gels, it is possible that the Ca-bearing mineralogical phases were stable at high pH levels, thereby minimizing the dissolution of Ca^{2+} ions to the solution. In this context, flexural strength only increased when exposed to accelerated carbonation, due to the reaction of OH^- from the alkaline activator with the Ca^{2+} ions released from the decalcified phases of EAFS to generate $Ca(OH)_2$ and subsequently $CaCO_3$.

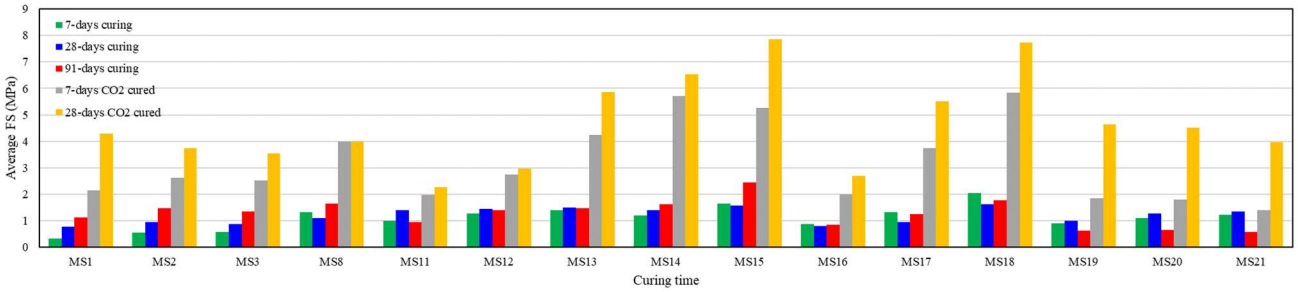

Figure 2 - Average flexural strength (FS)

3.4. CARBONATION

The specimens in this study, after 7 days exposure of CO_2, were considered fully carbonated, as there was no indication of a pinkish hue from the phenolphthalein pH indicator thereby making the CO_2 penetration immeasurable. Alkali-activated materials are known to present a fast decline in pH with ongoing polymerization reactions due to the consumption of the OH- ions present in the pore solution. This phenomenon, in combination with the carbonation of Ca-bearing phases, led to an overall decline of the specimens' pH.

The average compressive and flexural strengths of specimens subjected to accelerated carbonation were tested following EN 1015-11 [20]. A noticeable improvement in the mechanical performance of AAEAFS mortars was observed. The additional 28 days of accelerated carbonation led to a near 800% and 500% increase in compressive strength and flexural strength, respectively. The increase in compressive strength was from 3.9 MPa in uncarbonated mixes to 31 MPa in carbonated mixes. The flexural strength improved from 1.6 MPa to 7.85 MPa for the uncarbonated and carbonated samples, respectively. The maximum mechanical performance was obtained in mixes with 12% and 1.0 for Na_2O/binder and SiO_2/Na_2O ratios, respectively, thus showing a shift in the optimal alkaline activator contents. It is likely that Ca^{2+} ions were released from the EAFS' Ca-bearing phases and reacted with OH^- ions from the alkali activator, thereby producing $Ca(OH)_2$. This compound later reacted with the CO_2 forced into the microstructure, resulting in the precipitation in $CaCO_3$ polymorphs, which significantly densified the microstructure and thus increased strength [25, 30].

3.5. SHRINKAGE

In **Error! Reference source not found.**, the change in length (i.e. shrinkage) of sealed specimens with little to no humidity exchange with the surrounding environment was tested for 91 days. Most specimens presented considerable shrinkage, with one of them being close to 3500 µm/m, which is three times higher than typically observed for standard cement mortars. The water may have been mostly used in the alkali activation reaction, leading to a considerable autogenous shrinkage. No correlation with the alkali solution composition was observed. All specimens presented at least 45% of their total 91-day shrinkage in the first 28 days, except for mix MS8. This one slightly expanded, with minor fluctuations, for the first 28 days and started to shrink later on to settle at 198 µm/m after 91 days. This behaviour also occurred in fly ash (FA) mortars studied by Atiş et al. [36]. The authors hypothesized that the expansion of mortars containing FA could be from the MgO and the high content of SO_3, which can result in long-term instability due to the formation of expansive calcium sulphate phases [36]. Atiş et al. [36] also stated that materials having expansion properties could be implemented as 'shrinkage-reducing agents' by trial amounts to compensate for the shrinkage of cement elements [36].

4. CONCLUSIONS

In this study, electric arc furnace slag (EAFS) was examined as a potential full replacement of cement in the production of alkali-activated mortars. The results obtained in this campaign allowed concluding that EAFS as the sole precursor will result in mixes with low performance. This is most likely due to the lower amount of amorphous phases compared to other common aluminosilicate pozzolans. Regarding the alkali activator's optimal contents, it was found that the SiO_2/Na_2O ratio and compressive strength are generally directly proportional. The maximum recorded performance of specimens occurred for mixes with 4% and 2.5 for Na_2O/binder and SiO_2/Na_2O ratios, respectively. Another parameter affecting the compressive strength is time, thereby showing continued reaction after the 24 h

thermal curing stage. The specimens in this study experienced 7 days, 28 days, and 91 days of curing time in a dry chamber at 23 ± 2 ºC and relative humidity of 65%. The maximum recorded compressive strength was obtained at 91 days of curing (4% Na_2O/binder ratio and 2.5 SiO_2/Na_2O ratio). However, despite the shortcomings of EAFS as a sole precursor, the mechanical performance increased significantly after subjecting the specimens to an accelerated carbonation stage. After subjecting 28 days to a CO_2-enriched environment, the AAEAFS showed an average compressive strength increase of ~500%, with one case reaching 800% (i.e. from an initial 3.9 MPa in uncarbonated mixes to 31 MPa for carbonated ones). The maximum performance was observed in mixes with 12% and 1.0 for Na_2O/binder and SiO_2/Na_2O ratios, respectively, thus showing a shift in the optimal alkaline activator contents. The sealed shrinkage test showed considerable dimensional variability over time. Great autogenous shrinkage may have occurred due to the continuous alkali activation reaction. Nevertheless, this phenomenon is still widely unknown and must be further researched. The complete replacement of cement with alkali-activated aluminosilicate wastes may translate into significant reductions in cost and minimal environmental impacts, especially with incorporating a forced carbonation curing stage using industrial CO_2-rich flue gases. Therefore, greater focus should be given to this curing technique in further future research.

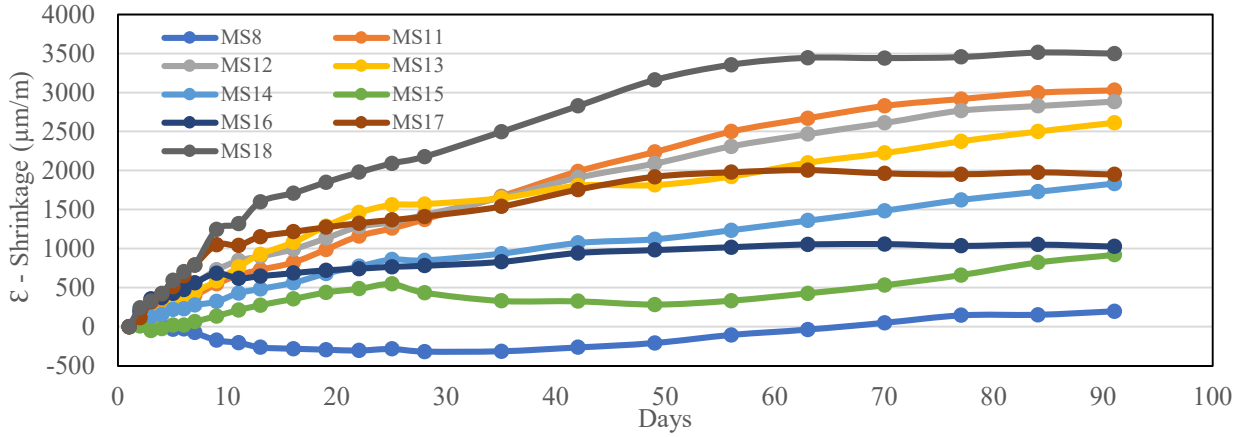

Figure 3 - Shrinkage

Acknowledgements

The authors acknowledge the support of the CERIS Research Institute, IST, University of Lisbon and FCT- Foundation for Science and Technology, through the research project PTDC/ECI- CON/29196/2017 "Recycled Inorganic Polymer Concrete: Towards a fully recycled and cement-free concrete" (RInoPolyCrete). The authors would also like to acknowledge the support of Valorsul, EDP and SIKA for part of the materials provided for this experimental campaign.

References

[1] Pellegrino, C.; Cavagnis, P.; Faleschini, F.; Brunelli, K., 2013. "Properties of concretes with black/oxidizing electric arc furnace slag aggregate", Cement and Concrete Composites 37, pp. 232-240.

[2] Jiang, Y.; Ling, T.-C.; Shi, C.; Pan, S.-Y., 2018. "Characteristics of steel slags and their use in cement and concrete—A review", Resources, Conservation and Recycling 136, pp. 187-197.

[3] Chunlin, L.; Kunpeng, Z.; Depeng, C., 2011. "Possibility of concrete prepared with steel slag as fine and coarse aggregates: A preliminary study", Procedia Engineering 24, pp. 412-416.

[4] Brazil Sustainability Institute, 2018. "Sustainability Report", http://acobrasil.org.br/sustentabilidade/eng/. (Accessed 2021).

[5] Arribas, I.; Vegas, I.; San-Jose, J. T.; Manso, J. M., 2014. "Durability studies on steelmaking slag concretes", Materials & Design 63, pp. 168-176.

[6] Manso, J. M.; Polanco, J. A.; Losanez, M.; Gonzalez, J. J., 2006. "Durability of concrete made with EAF slag as aggregate", Cement and Concrete Composites 28(6), pp. 528-534.

[7] Papayianni, I.; Anastasiou, E., 2010. "Production of high-strength concrete using high volume of industrial by-products", Construction and Building Materials 24(8), pp. 1412-1417.

[8] Češnovar, M.; Traven, K.; Horvat, B.; Ducman, V., 2019. "The potential of ladle slag and electric arc furnace slag use in synthesizing alkali activated materials; the influence of curing on mechanical properties", Materials 12(7), 1173 p.

[9] Blengini, G., 2006. "Life cycle assessment tools for sustainable development: case studies for the mining and construction industries in Italy and Portugal", Technical University of Lisbon, Portugal.

[10] Braga, A., 2015. "Comparative analysis of the life cycle assessment of conventional and recycled aggregate concrete Instituto Superior Técnico", University of Lisbon, Portugal.

[11] Chen, C.; Habert, G.; Bouzidi, Y.; Jullien, A.; Ventura, A., 2010. "LCA allocation procedure used as an incitative method for waste recycling: An application to mineral additions in concrete", Resources, Conservation and Recycling 54(12), pp. 1231-1240.
[12] De Schepper, M.; Van den Heede, P.; Van Driessche, I.; De Belie, N., 2014. "Life cycle assessment of completely recyclable concrete", Materials 7(8), pp. 6010-6027.
[13] Marinković, S.; Radonjanin, V.; Malešev, M.; Ignjatović, I., 2010. "Comparative environmental assessment of natural and recycled aggregate concrete", Waste Management 30(11), pp. 2255-2264.
[14] Ozturk, M.; Akgol, O.; Sevim, U. K.; Karaaslan, M.; Demirci, M.; Unal, E., 2018. "Experimental work on mechanical, electromagnetic and microwave shielding effectiveness properties of mortar containing electric arc furnace slag", Construction and Building Materials 165, pp. 58-63.
[15] Hafez, H.; Kassim, D.; Kurda, R.; Silva, R. V.; de Brito, J., 2021. "Assessing the sustainability potential of alkali-activated concrete from electric arc furnace slag using the ECO2 framework", Construction and Building Materials 281, 122559.
[16] Arribas, I.; Santamaria, A.; Ruiz, E.; Ortega-Lopez, V.; Manso, J. M., 2015. "Electric arc furnace slag and its use in hydraulic concrete", Construction and Building Materials 90, pp. 68-79.
[17] Europeia, U., 1998. "Diretiva 98/83/CE do Conselho, de 3 de novembro de 1998, relativa à qualidade da água destinada ao consumo humano", Jornal Oficial das Comunidades Europeias. L 330, pp. 32-54.
[18] EN-196-1, 2005, "Methods of testing cement - Part 1: Determination of strength", Comité Européen de Normalisation (CEN), Brussels, Belgium, 36 p.
[19] EN-1015-3, 1999, "Methods of test for mortar for masonry - Part 3: Determination of consistence of fresh mortar (by flow table)", Comité Européen de Normalisation (CEN), Brussels, Belgium, 10 p.
[20] EN-1015-11, 1999, "Methods of test for mortar for masonry - Part 11: Determination of flexural and compressive strength of hardened mortar", Comité Européen de Normalisation (CEN), Brussels, Belgium, 12 p.
[21] EN-13295, 2004, "Products and systems for the protection and repair of concrete structures.Test methods. Determination of resistance to carbonation", Comité Européen de Normalisation (CEN), Brussels, Belgium, 18 p.
[22] EN-1015-13, 1993, "Methods of test for mortar for masonry - Part 13: Determination of dimensional stability of hardened mortars", Comité Européen de Normalisation (CEN), Brussels, Belgium, 20 p.
[23] Fernández-Jiménez, A.; Puertas, F., 2001. "Setting of alkali-activated slag cement. Influence of activator nature", Advances in Cement Research 13(3), pp. 115-121.
[24] Türker, H. T.; Balçikanli, M.; Durmuş, İ. H.; Özbay, E.; Erdemir, M., 2016. "Microstructural alteration of alkali activated slag mortars depend on exposed high temperature level", Construction and Building Materials 104, pp. 169-180.
[25] Ozturk, M.; Bankir, M. B.; Bolukbasi, O. S.; Sevim, U. K., 2019. "Alkali activation of electric arc furnace slag: Mechanical properties and micro analyzes", Journal of Building Engineering 21, pp. 97-105.
[26] Peys, A.; Arnout, L.; Blanpain, B.; Rahier, H.; Van Acker, K.; Pontikes, Y., 2018. "Mix-design parameters and real-life considerations in the pursuit of lower environmental impact inorganic polymers", Waste and Biomass Valorization 9(6), pp. 879-889.
[27] Abdollahnejad, Z.; Jesus, C. M.; Pacheco-Torgal, F.; Aguiar, J., 2013. "One-part geopolymers versus Ordinary Portland Cement (OPC) mortars: durability assessment", 2nd International Conference on Wastes: "Solutions, Treatments and Opportunities", pp. 115-120.
[28] Bernal, S. A.; Provis, J. L.; Rose, V.; Mejía de Gutierrez, R., 2011. "Evolution of binder structure in sodium silicate-activated slag-metakaolin blends", Cement and Concrete Composites 33(1), pp. 46-54.
[29] Shearer, C. R.; Provis, J. L.; Bernal, S. A.; Kurtis, K. E., 2016. "Alkali-activation potential of biomass-coal co-fired fly ash", Cement and Concrete Composites 73, pp. 62-74.
[30] Song, S.; Jennings, H. M., 1999. "Pore solution chemistry of alkali-activated ground granulated blast-furnace slag", Cement and Concrete Research 29(2), pp. 159-170.
[31] Wang, S.-D.; Scrivener, K. L.; Pratt, P., 1994. "Factors affecting the strength of alkali-activated slag", Cement and Concrete Research 24(6), pp. 1033-1043.
[32] Gu, Y.-m.; Fang, Y.-h.; You, D.; Gong, Y.-f.; Zhu, C.-h., 2015. "Properties and microstructure of alkali-activated slag cement cured at below-and about-normal temperature", Construction and Building Materials 79, pp. 1-8.
[33] Caijun, S.; Yinyu, L., 1989. "Investigation on some factors affecting the characteristics of alkali-phosphorus slag cement", Cement and Concrete Research 19(4), pp. 527-533.
[34] Criado, M.; Fernández-Jiménez, A.; De La Torre, A.; Aranda, M.; Palomo, A., 2007. "An XRD study of the effect of the SiO2/Na2O ratio on the alkali activation of fly ash", Cement and Concrete Research 37(5), pp. 671-679.
[35] Qureshi, M. N.; Ghosh, S., 2014. "Effect of silicate content on the properties of alkali-activated blast furnace slag paste", Arabian Journal for Science and Engineering 39(8), pp. 5905-5916.
[36] Atiş, C. D.; Kilic, A.; Sevim, U. K., 2004. "Strength and shrinkage properties of mortar containing a nonstandard high-calcium fly ash", Cement and Concrete Research 34(1), pp. 99-102.